Development of Radiation-Hard Solid-State Amplifiers for kilo-Gray Environments using COTS components

Chihiro Ohmori, Mauro Paoluzzi

***Abstract*—The High-Luminosity LHC (HL-LHC) project is the upgrade of the LHC to increase its luminosity by a factor of five compared to the nominal value. The LHC Injector Upgrade (LIU) project aims at upgrading the LHC injector chain to reach the goal of HL-LHC. The LIU project covers all injectors, that is, the new Linac 4, PS Booster (PSB), PS and SPS. In the PSB, the present ferrite-loaded RF accelerating systems will be replaced with new magnetic alloy (Finemet®) loaded cavity systems. The new cavity system allows the implementation of a cellular topology and the use of solid-state RF power amplifiers. The PSB will have 144 cavity cells and amplifiers, and each amplifier uses 17 high power MOSFETs. The new RF systems will be installed in the straight sections where the total ionization dose (TID) is 20 Gy/year, which may even increase after the upgrade. R&D work has been performed to validate the use of solid-state amplifiers in this radioactive environment. In this paper, we describe a novel technique to stabilize the solid-state amplifier up to the total dose of about 10 kGy. This technique will enable the use of solid-state amplifiers in even higher radiation environments**

***Index Terms*—Proton Synchrotron, Wideband RF Acceleration System, Solid State Amplifier, MOSFET, single-event effect (SEE), total ionization dose (TID), Commercially Off The Shelf (COTS)**

I. INTRODUCTION

THE LIU project [1], [2] includes upgrade and consolidation of RF system of the LHC injector chain to get ready for HL-LHC [3]. The present PSB RF system consists of three different systems to cover the bandwidths for beam acceleration on h=1, the 2^{nd} harmonic RF and higher harmonic RF for controlled longitudinal emittance blow-up [4]. These systems occupy 4 straight sections in the booster. The new Magnetic Alloy loaded system [5] using Finemet® [6], [7] will be installed in the straight sections, and its large instantaneous bandwidth (0.5 MHz to 20 MHz) covers the frequency band of all required harmonics [8]. Due to this replacement, one straight section will be freed. Fig. 1 shows an RF system for one straight section. As the PSB consists of 4 superposed accelerator rings, the RF system consists of 4 stacked systems. The radiation levels in these straight sections are about 20 Gy/year. So far, solid-state amplifiers using a 300 W MOSFET have been employed in the prototype Finemet® RF system, with the amplifiers directly connected to the accelerating gap and sit near the RF cavity.

Manuscript received March 11, 2019

Chihiro Ohmori is with the J-PARC Center, JAEA & KEK, 2-4 Shirakata, Tokai, Ibaraki 319-1195, Japan. (e-mail: chihiro.ohmori@kek.jp)

Mauro Paoluzzi is with CERN, CH-1211 Geneva 23 Switzerland. (e-mail:mauro.paoluzzi@cern.ch)

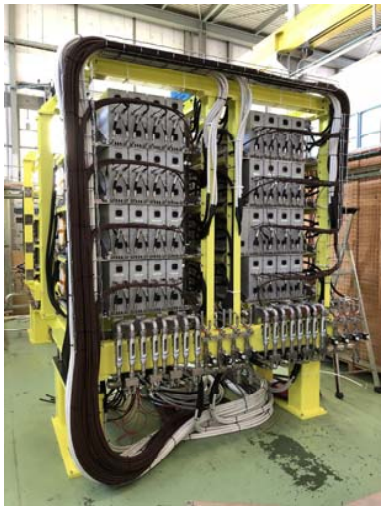

Fig. 1. CERN PSB Cavities and Solid-State Amplifiers before installation.

LIU also includes a substantial increase of the PS beam intensity to be injected into the SPS. In the PS, longitudinal coupled bunch instabilities are observed [9] and could be damped by means of a spare RF cavity up to the beam intensity of $1.3 \times 10^{11}\mathrm{ppb}$. A wideband longitudinal RF damper has been installed in the PS to go above this intensity as shown in Fig. 2 [10] and damp simultaneously many different coupled bunch modes [11]. So far, $2.6 \times 10^{11}\mathrm{ppb}$ have been injected into the SPS as required by the project baseline. Here again, to drive the wideband magnetic alloy RF system, solid-state amplifiers are used in a configuration that is similar to that adopted in the PSB. Since the radiation dose in the chosen PS area is about $1\ \mathrm{kGy/year}$ [12], the solid-state amplifiers are installed with an iron shielding as shown in Fig. 2.

The further reduction of the equivalent impedance presented by the RF cavities to the circulating beams can be achieved by increasing the gain of the fast feedback loop in the PS RF systems, as in the 10 MHz cavities shown in Fig. 3 [13]. The goal is to mitigate the beam loading effects of the high intensity beams. So far, tube amplifiers have been used in the fast feedback chain because of the high radiation level [14], reaching the limit allowed by this technology [13]. A further increase of feedback gain could be envisaged

Fig. 2. CERN PS Longitudinal Damper Cavity with Iron Shielding underneath for Solid State Amplifiers

Fig. 3. CERN PS Ferrite-loaded Cavity driven by the tube amplifier. A feedback amplifier is used for beam loading compensation and higher gain is required to cope with larger intensity.

only by employing a solid-state amplification stage. Increased gain requires small group delay, which is possible only with the feedback amplifier near the cavity, where extra shielding can hardly be added to protect the amplifier from radiation damage. A radiation-hard solid-state amplifier fitting the high radiation environment of the PS tunnel would therefore be mandatory.

CERN and KEK/J-PARC have been cooperating to develop the wideband Finemet® based RF systems for the PSB and PS since 2012. The collaboration also included the test and development of radiation-hard, solid-state amplifiers using Commercial Off-The-Shelf (COTS) components. Tests were carried out in radiation environments of the three institutes as well as in other irradiation facilities. In this paper, we describe the strategy followed to choose MOSFETs for the PSB RF system and the developments performed to improve the radiation hardness of our devices. We also report recent developments of the radiation-hard solid-state amplifier for the high radiation environment of 8.8 kGy.

TABLE I
LIST OF MOSFETS

type	geometry	manufacture	V_{DSS}
MRF151	VMOS	M/A com	125 V
SD2942	VMOS	ST Microelectronics	130 V
MRF151	VMOS	Motorola	discontinued
VRF151	VMOS	Microsemi	170 V
MRFE6VP6300	LDMOS	Freescale	130 V

II. DEVELOPMENTS OF RAD-HARD SOLID-STATE AMPLIFIERS FOR THE PSB

A. Choice of MOSFET

In 2013, when the CERN accelerators were stopped during the first long shutdown, LS1, the first irradiation test of several power MOSFETs was carried out in the J-PARC Main Ring (MR) as listed in Table I. The MOSFETs of 300 W class were mounted on the PCB and installed at the downstream of the collimator as shown in Fig. 4. In the J PARC MR, the beam loss is localized at the collimator position. Although the collimator is surrounded by an iron shielding, the scattered particles escape through the beam pipe and hit the MOSFETs on the PCB. The radiation dose was measured by the RadMon system developed at CERN [15]. Because the MR is a proton synchrotron, the test area is a mixed field of radiations including gammas, charged particles and neutrons. The rate of TID was 250 Gy/day after adjustment of the collimator. The RadMon worked up to 4.2 kGy. As shown in Fig. 5, the TID is proportional to the number of protons. After the RadMon stopped working, the total dose was estimated from the total number of protons. During the test, a 15 kW beam was delivered to the slow extraction during 10 days, followed by a 200 kW beam delivered to the T2K experiment. In total, a TID of 12 kGy and an integrated neutron flux of $7.2 \times 10^{13}\mathrm{n/cm^2}$ (1 MeV-equivalent) were provided during the irradiation. The ratio between the TID and the neutron flux was $0.60 \times 10^{13}\mathrm{n/cm/kGy}$ at the J-PARC MR. The irradiation test also aimed at assessing the risk related to Single Event Effects, SEE, on the high power MOSFETs in view of their use in hadron accelerators. In the PSB, VMOS- type MOSFETs have been used for decades in the feedback amplifiers of the final stage of the RF acceleration systems. The possibility of Single Event Burnout, SEB, and Single Event Gate Rupture, SEGR, were pointed out for the use of high power MOSFETs [16], [17], and their destructive effects were indeed observed. For their evaluation, the MOSFETs were placed in parallel to the beam to mimic the amplifiers in the PSB tunnel.

The control system of the devices was located in the power supply building which is about 200 m away from the setup. A drain voltage of 48 V was applied for each MOSFET. The gate voltage of each MOSFET was ramped from 0 to 10 V in 1 ms to measure the drain current. Fig. 6 shows the pattern of gate voltage and drain current of each MOSFET. The drain currents were measured every hour. Before the measurements, the control system checked the status of each MOSFET. Fig. 7 shows the results of the irradiation test. The radiation effects on the MOSFET appeared as the drifts of the gate bias voltage. Fig. 7 shows the variations of bias voltage for the drain current

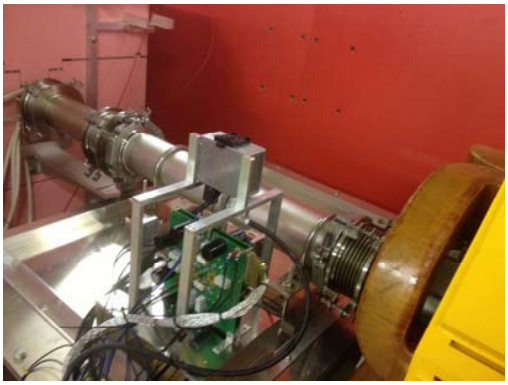

Fig. 4. The test setup on the PCB was installed downstream of the collimator (Left) in the J-PARC MR. The radiation dose and neutron flux were measured by the RadMon Systems.

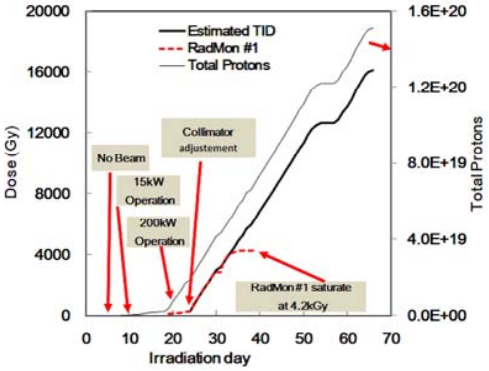

Fig. 5. The TID and number of protons during the MOSFET test at the J-PARC. RadMon #1 which is on the MOSFETs is used as a reference of the dose which MOSFETs were received. Expected dose was calculated from total protons.

of 1 A. The vertical-style MOSFETs, VMOS, show a larger variation, while LDMOS show less variation. All MOSFETs survived a dose in excess of 2 kGy, which corresponds to many years of operation in the PSB. No failures caused by SEE were measured up to 2 kGy. As shown in Table I, these MOSFETs have different drain-source breakdown voltage.

The solid-state amplifiers in the PSB will drive the cavity directly and large voltages are expected to be induced by the circulating beam. The MOSFET VRF151, a Vertical Double-diffused MOS, VDMOS-type, which has the largest V_{DSS}, was selected for the final stage amplifiers in the PSB. The large V_{DSS} also ensures a large voltage de-rating which is known to limit the devices sensitivity to SEE [18].

B. Mitigation of Radiation

After the irradiation test at J-PARC, the test was continued at Fraunhofer Institute using the gamma-rays of ^{60}Co. Fig. 8 shows the behaviour and variation of bias characteristics of 8 MOSFETs of type VRF151. All of them show the same behaviour before and after the irradiation of 3 kGy. The gate threshold voltage for the drain current of 1 A drops to 20%

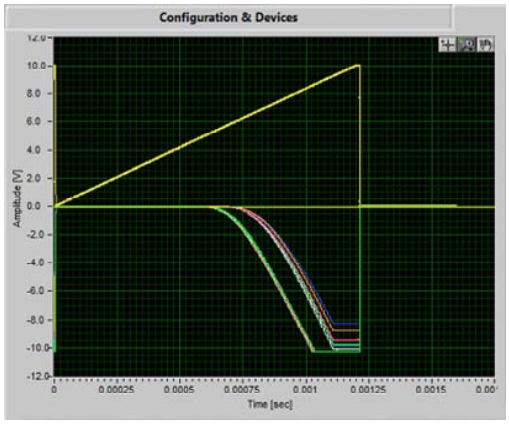

Fig. 6. The display on the online monitor. The gate voltage is ramped in mili-second (upper line). The drain currents of MOSFETs are measured (lower lines) and 1 V of amplitude corresponds to 1 A of the drain current of each MOSFET.

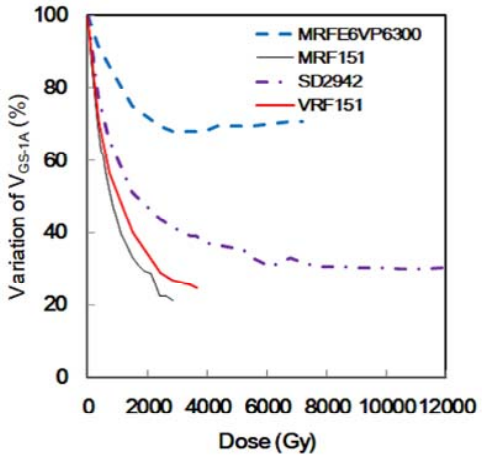

Fig. 7. The results of the irradiation test of MOSFETs at the J-PARC MR in 2013. The radiation effects on 4 different MOSFETs are shown as variations of gate threshold voltages for the drain current of 1 A.

of the initial value, consistent with the results obtained at J-PARC (Fig. 7). It is the TID effect on the power MOSFET. Although the TID effects are less problematic in digital and high-performance analogue CMOS technologies because SiO_2 gate dielectric layers are thin, power MOSFETs still need thickness to stand high drain-source voltage, V_{DSS} [19], [20], [21].

As the radiation effects seem reproducible, a mitigation test was carried out. It used a sensing device to generate a reference gate voltage proportional to its threshold voltage,V_{TH}. The reference voltage was then applied to all amplifier devices, thus collectively compensating changes due to radiations. Three MOSFETs were tested using a sensing device. The results are shown in Fig. 9. A MOSFET without the mitigation shows rapid variation of bias characteristics. As the drain current increases rapidly, the power dissipation will become inacceptable. The other three MOSFETs with the mitigation

show stable behaviours and survived up to 2 kGy.

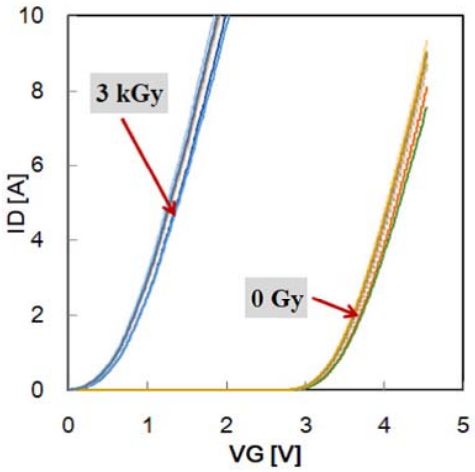

Fig. 8. Irradiation test of MOSFETs, VRF151, at Fraunhofer Institute. In the test, 8 MOSFETs were tested and all show the same behavior before and after 3 kGy irradiation.

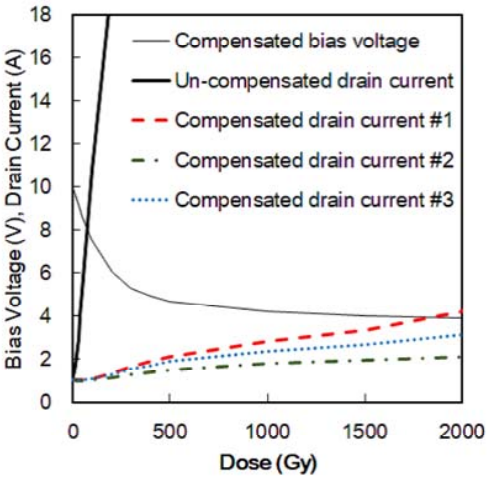

Fig. 9. Mitigation test of MOSFETs, VRF151, at Fraunhofer. It shows that the drain currents were stabilized by applying the compensated bias voltage on the gate of each MOSFET.

C. Radiation Environments in the PSB

The radiation level in the straight sections available for installation of the new RF systems in the PSB tunnel was measured using the RadMon system. The highest radiation dose, found in section 10L1, is about 20 Gy/year. It may become slightly larger after full implementation of LIU. This value is 2 to 5 times higher than in the other available sections and corresponds to a sufficiently long lifetime of the VRF151 MOSFET (many years of operation).

D. Power Test under the radiation

It is known that the radiation effects on MOSFETs also depend on temperature and operation conditions. We prepared a setup to test solid-state amplifiers under radiation condition. Fig. 10 shows the amplifier located near the ^{60}Co source. During the irradiation test, the amplifier generated 100 W of RF power sweeping the frequency from 0.5 MHz to 5 MHz. MOSFET #1, used in the amplifier, was mounted on an aluminium heat sink and was cooled by a cooling fan. Next to the amplifier, MOSFET #2 was mounted on another cooling unit to monitor the radiation effect. The gate voltage was adjusted to allow constant current flow to the MOSFET #2 and the same gate voltage was supplied to MOSFET #1 in the amplifier to mitigate the radiation effects. An Auto Level Control (ALC) loop was used to stabilize the RF output to 100 W. A dummy load was mounted behind MOSFET #2 and was cooled by the fin and fan. The RF power was monitored and the monitor signal was sent to the ALC circuit. The circuit diagram of the system is shown in Fig. 11.

Fig. 10. Irradiation test of solid-state amplifiers (left) at QST-Takasaki. The ^{60}Co source will be inserted in the tube of wire mesh (right). The other setups for MOSFETs test are also shown

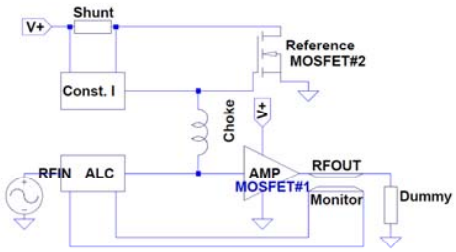

Fig. 11. The circuit diagram of 120 W amplifier with the mitigation circuit.

We prepared 2 amplifiers setups. They were located at 15 Gy/hr and 2 Gy/hr. The dose was measured by Aminogray, Alanine dosimeter. The amplifiers were irradiated for 160 hours in total, resulting in accumulated doses of 2.4 kGy and 320 Gy, respectively. Both amplifiers were driven during the irradiation test with 100% duty factor. The RF frequency was swept with 2 min. cycle. The RF amplitudes of input and output were rectified and recorded using a data logger. The RF phases of the RF outputs were detected by the phase

detector. The gate voltage to mitigate the radiation effects for both amplifiers showed same behaviour of the radiation.

The results of the radiation test are shown in Fig. 12. Both setups survived and variations of the amplifier gain between 0.5 MHz and 5 MHz were about 1 dB. Fig. 13 shows the gain variation at 0.5 MHz. Both, Figs. 12 and 13 show that the gain variation occurs at the beginning of the irradiation below 300 Gy. When using solid-state amplifiers to drive the RF cavities, a gain variation of about 1 dB is acceptable because an ALC loop is usually used to stabilize the RF voltage. Although gain variations were observed, a variation of phase was not observed during the test.

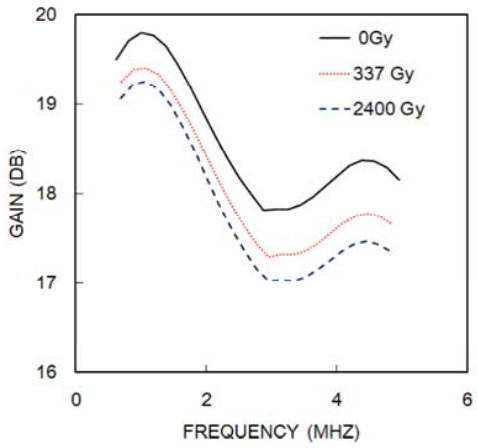

Fig. 12. Variation of the amplifier gain by the gamma-ray radiation. The amplifier was irradiated with the dose rate of 15 Gy/hr for 160 hours.

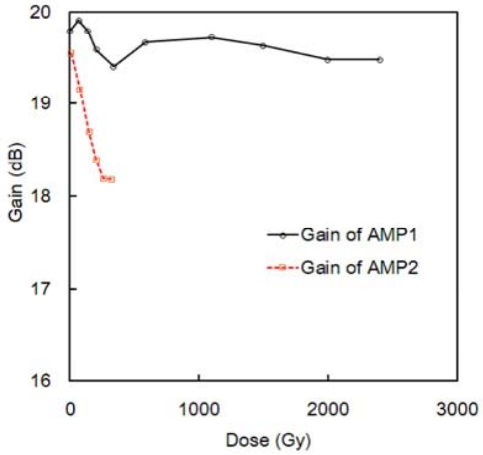

Fig. 13. Variations of the amplifier gains at 0.5 MHz. The gain variations occurred at lower dose.

E. Mixed-Field Radiation test at the CHARM facility

Following the tests at QST-Takasaki, the solid-state amplifier was shipped to CERN for testing at the CERN High

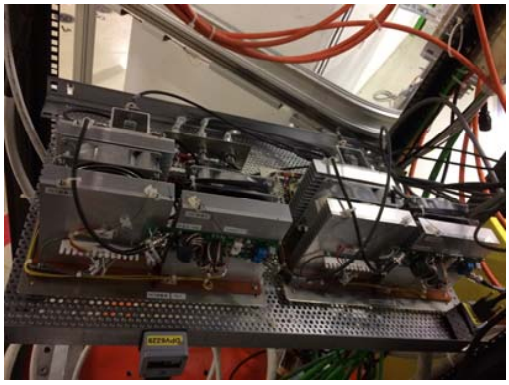

Fig. 14. Setup for the test at the CHARM facility. Amplifiers with VRF151G (left) and LDMOS (right) were tested.

energy AcceleRator Mixed-field facility (CHARM) [22], [23]. CHARM uses the proton beam of the PS. Particles scattered from a Cu target, including gamma-rays, charged particles, neutrons and other hadrons, will hit the components under test. Total ionization dose and neutrons are measured by the RadMon, which was placed near the amplifiers [24]. The solid-state amplifiers before installation are shown in Fig. 14. Another amplifier using LDMOS was also tested as described in the next section. The scattered particles hit the amplifiers from the front, perpendicularly. The irradiation test was carried out for 3 weeks and total number of 5.25×10^{16} protons were delivered.

Fig. 15 shows the results under the mixed field radiation at CHARM [25]. The amplifier using VRF151 survived until the end of the experiment. A total dose of 1.9 kGy and neutron flux of $1.1 \times 10^{13}\mathrm{n/cm}$ were delivered. The variation of the gain due to the radiation was about 1 dB as shown in Fig. 15 and it is consistent with the result at QST-Takasaki shown in Fig. 12. These results suggest that the variation of the amplifier gain using VRF151 is dominated by the total dose effect and it does not depend on the flux of neutrons and other particles. At CHARM, the ratio of the total ionization dose and neutron flux is $0.57 \times 10^{13}\mathrm{n/cm^2/kGy}$. It is interesting that the ratio is almost same as the number of the J-PARC MR collimator section ($0.60 \times 10^{13}\mathrm{n/cm^2/kGy}$) although the beam loss at the J-PARC occurred around 3 GeV and CHARM uses a 27 GeV proton beam. Fig. 16 shows the gain variation of the solid-state amplifier at 0.5 MHz. It shows the gain variation occurred below 300 Gy. It is also consistent with the irradiation with the gamma ray as shown in Fig. 13.

F. Effect of the position with respect to beam line and reference MOSFET

A 3 kW solid-state amplifier was installed in the CERN PS to observe the effect of different MOSFET positions with respect to the beam line and the reference MOSFET on the compensation. An amplifier was placed right under the PS damper without any radiation shielding (Fig. 2). It used 18 MOSFETs, including one for the driver and another as the reference for the compensation. The driver and radiation

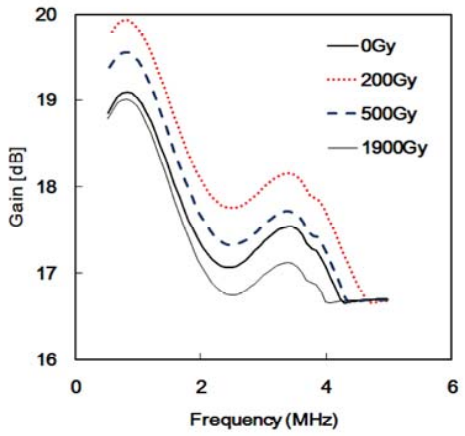

Fig. 15. The gain variation under the mixed field radiation at the CHARM. Because of the shortage of RF input of the 120 W amplifier, the gain at the frequency higher than 4 MHz was not measured properly after 1.9 kGy irradiation because of the shortage of input power.

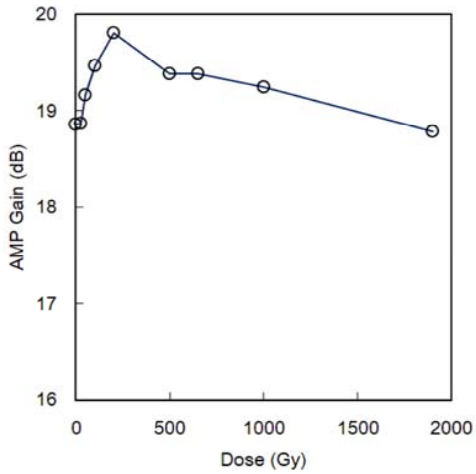

Fig. 16. The gain variation at 0.5 MHz under the mixed field radiation at the CHARM.

reference MOSFETs were placed in the centre of the amplifier. The 16 other devices were placed in couples vertically above and below as sketched in Fig. 17, which also indicates the beam line position. It also shows the variation of the drain current of the 16 MOSFETs during the deposition of the first 50 Gy. It can be seen that the devices closer to the beamline than the reference MOSFET were undercompensated, while the compensation of those on the same level or below was reasonably good. This can be explained by a higher dose deposition on the closer devices. This assumption was verified by turning the amplifier upside down, thus inversing the device distance from the beam line. Fig. 18 shows the result of the irradiation test to about 70 Gy and, as expected, the current variation rates inverted with the amplifier mounted upside down. The locations of the MOSFETs are shown on

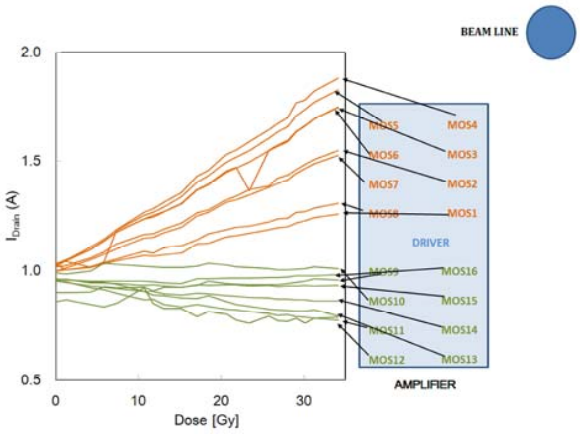

Fig. 17. The effect of position. A 3 kW solid-state amplifier was set below the damper cavity without any radiation shielding. The drain current of each MOSFET were measured showing position dependence.

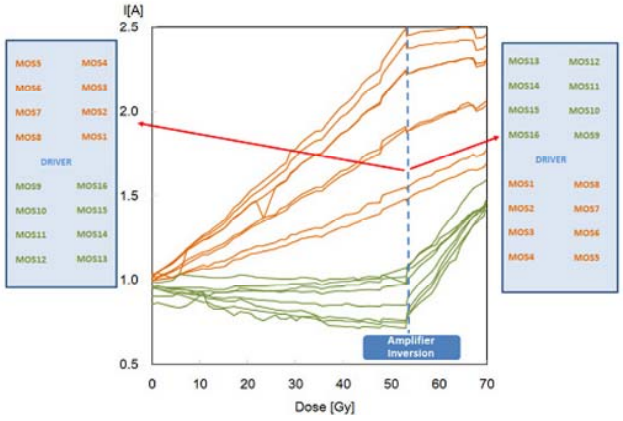

Fig. 18. After turning the amplifier upside down, the compensation effects on the devices also inverted.

the right side. The reference MOSFET for the compensation was located beside the driver MOSFET. It clearly shows that the MOSFETs in the upper side of the amplifier had large drift because the compensation was not enough. The other MOSFET in the lower side show the over-compensation. It can be explained by the upper half receiving more dose than the reference MOSFET while the lower set received less dose.

G. *Evaluations for the usages*

In the PSB, the dose rate is much smaller than in the PS, and it is expected that the effect of the MOSFET position will occur slowly. Fig. 17 suggests however that the compensation scheme using one reference MOSFET is not perfect. Fortunately, synchrotrons typically have an RF-off period, when the beam is extracted and the magnets ramp down. A new scheme using the idling currents of all MOSFETs to adjust each gate voltage during this RF-off period can thus be envisaged.

The irradiation tests using ^{60}Co and mixed field show that the solid-state amplifier using VRF151 survives up to 2 kGy. So far, no failure was observed, neither single event effects, SEE, nor otherwise. The dose of 2 kGy corresponds to about 100 years of operation in todays PSB.

Moreover, the solid-state amplifiers for the PS damper system, which are protected by the iron shielding as shown in Fig. 2, will receive 50 times less dose than the outside of the shielding as shown in Fig. 19. It can thus be expected that the solid-state amplifiers for the damper system also have an acceptable lifetime.

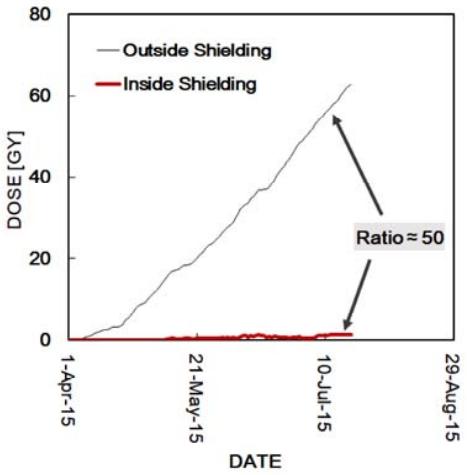

Fig. 19. The dose inside and outside of the iron shielding.

III. DEVELOPMENTS OF RAD-HARD SOLID-STATE AMPLIFIERS FOR THE PS ENVIRONMENT OF 1 KGY/YEAR

A. Radiation test of VMOS for 10 kGy environments

The solid-state amplifiers using vertical-type VDMOS, VRF151, satisfy the requirements for use in the PSB tunnel. With iron shielding, it is also possible to use them in the PS ring. However, tests at higher dose are required to qualify them for use in the PS ring without shielding. The feedback amplifiers in the final stage under the 10 MHz cavities require the robustness for the high radiation dose of several kGy.

Another irradiation test using ^{60}Co was carried out at QST-Takasaki. Fig. 20 shows the variation of the amplifier gain exposed to 8830 Gy, measured by the Aminogray. The MOSFET, VRF151, shows the variation of the gain of about 1 dB. It is about the same as in the irradiation tests at QST-Takasaki and CHARM as shown in Figs. 12 and 15. The results suggest that solid-state amplifiers can be used for the feedback chain of the 10 MHz RF systems. The use of the solid-state amplifiers will improve the feedback gain [13].

B. Radiation test of LDMOS

The Laterally Diffused Metal Oxide Semiconductor, LDMOS, is also used for RF power amplifiers. The radiation test

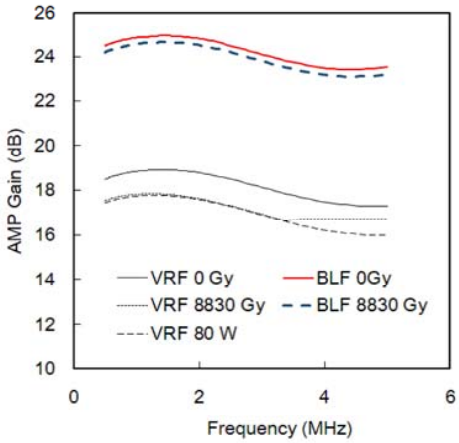

Fig. 20. The variation of the gain after exposure to 8830 Gy. Because of the shortage of RF input of the 120 W amplifier, the gain at the frequency higher than 3.5 MHz was not measured properly. The gain was also measured with the output power of 80 W.

at the J-PARC MR suggests that the LDMOS might be less sensitive to the radiation as shown in Fig. 7. Although the V_{DSS} is low as listed in Table I, the use of the feedback may still be possible as it is not affected by the beam directly.

A 500-W-class LDMOS was assembled in a push-pull, class AB amplifier and tested at QST-Takasaki. In the test, the compensation scheme adopting the circuit as shown in Fig. 11 was used. To improve the compensation, the MOSFETs for reference and in the amplifier were located close together. The results are also shown in Fig. 20. The amplifier using the LDMOS worked well until the end, and the gain variation is much less than in the VMOS amplifier.

The LDMOS amplifier was also tested at CHARM in 2017 as shown Fig. 14, exposed to a total dose of 1.9 kGy. The results are shown in Fig. 21. The gain drop started already below 650 Gy and a failure occurred. The behaviours were very different from the VDMOS as shown in Fig. 15. SEE is suspected as the cause of the failure.

The test of the LDMOS was repeated at CHARM in 2018. In total, a TID of 1150 Gy and a neutron flux of $9.3 \times 10^{12} \mathrm{n/cm^2}$ were irradiated on the sample. The amplifier setup is shown in Fig. 22. The amplifier was mounted on a heat sink for cooling. It was operated at 100 W fixed output power in pulsed mode. The frequency was swept from 0.5 MHz to 5 MHz. The pulse length was 9.5 s and the repetition time 10 s for the first 170 hours, then 20 s. Fig. 23 shows the compact controller which is developed for the PSB. It is used to adjust the gate bias to the constant drain current when the RF is off. The scheme is shown in Fig. 24. The quiescent current was set to 1 A total (0.5 A per MOSFET). The results plotted in Fig. 25 show that the gate bias, starting from 1.7 V initially lowered as the TID built up. After about 90 hours (320 Gy) a sudden quiescent current drop was recovered by the controller that increased the gate bias to 4 V following a failure caused by SEE.

Measurement of the MOSFETs characteristics at the end of the test showed that the gate-source resistance dropped to a few tens of Ω. With this low value the controller, designed to work on kΩ loads, could not maintain the correct biascondition. The resistance change happened in steps as shown by the gate voltage stepped changes (Fig .25) suggesting occurrence of SEE. Using RF drive, the devices trans-conductance was measured (Fig. 26) and it is showing a threshold displacement as well as a 35%-45% reduction. Comparing with Fig. 8, the variation of the trans-conductance may explain the gain reduction of LDMOS amplifier.

Another test on LDMOS was also carried out at PSI supporting the conclusion that the cause of the failures in the mixed radiation field was the SEE [26]. It is thus understandable that the variation of trans-conductance could not be compensated by shifting the gate voltage.

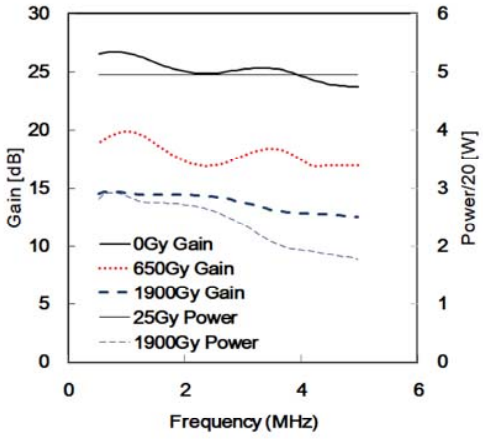

Fig. 21. The variations of the amplifier gain and output power by 1.9 kGy irradiation at CHARM. The output power also reduced to 40 W by the mixed field irradiation.

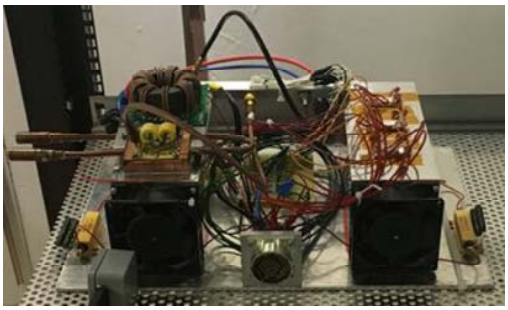

Fig. 22. Set up of an amplifier using LDMOS (left) and other system for DC operation (right).

IV. DISCUSSIONS

A. Mitigation Schemes

In the case of RF applications for particle accelerators, the idling currents of MOSFETs can be measured after beam extraction from the accelerator during RF-off. Therefore, real-time compensation can be applied during the accelerator operation. The mitigation scheme is unique and different from those used in the space applications [27], which adopt the variation of pulse width for adjusting the gate voltage to mitigate the TID effects, as well as a low noise amplifier [28] with a performance tuning algorithm.

Fig. 23. A compact gate bias controller developed for the PS booster new RF system.

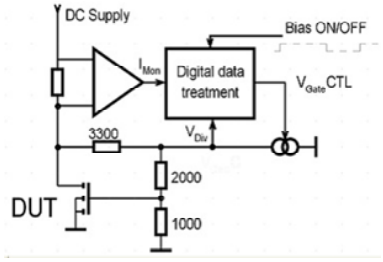

Fig. 24. Schematics for the constant drain rest current to mitigate the radiation effects. Beam OFF timing is used to measure the rest current and to adjust the gate voltage of the MOSFET.

B. Application to Medical Synchrotrons

In many proton and heavier ion synchrotrons for cancer treatments, magnetic alloy cavities are used [29], [30]. These cavities are driven by solid-state amplifiers located at a significant distance to protect them from radiation. However, there is a reflection and impedance mismatch problem when connecting coaxial cables between the cavity and amplifier. The developments of radiation-hard solid-state amplifiers using mitigation schemes can be used to locate the amplifier next to the cavities. The expected TID in medical accelerators is much lower than 10 kGy.

V. SUMMARY AND OUTLOOK

Rad-hard solid-state amplifiers using commercial off-the-shelf components were developed for use in kilo-Gray mixed-

TABLE II
PARAMETERS OF MOSFETS

type	geometry	manufacture	V_{DSS}	Output	Typ. Gain	applications
VRF151	VDMOS	Microsemi	170 V	300 W	18 dB	Final Stage AMP
BLF574	LDMOS	NXP	110 V	500 W	24 dB	feedback AMP

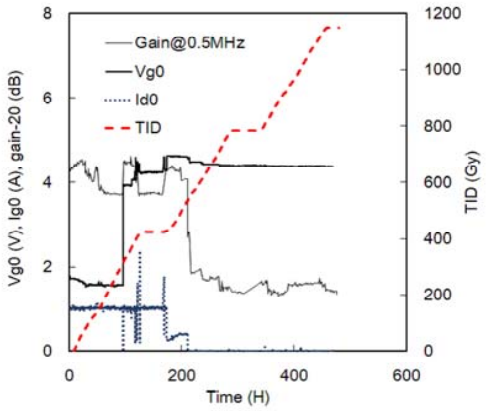

Fig. 25. The variation of the amplifier gains, gate voltage, idling drain current and TID. In total, TID of 1.1 kGy and $9.3 \times 10^{12}\mathrm{n/cm^2}$ were irradiated on the amplifier using LDMOS.

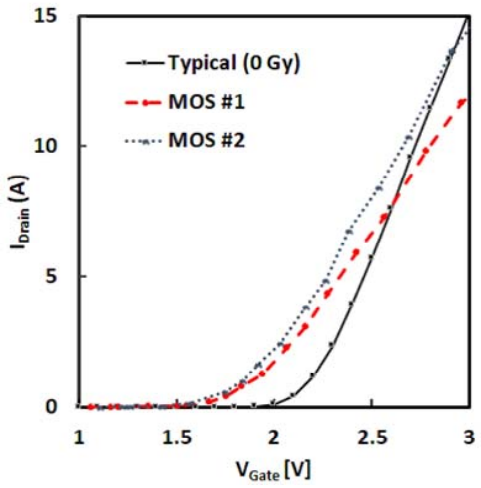

Fig. 26. Variation of Device trans-conductance of LDMOS before and after irradiation.

field environments. The mitigation scheme to compensate the total ionization dose effects works well for VDMOS-type MOSFETs up to a total dose of 8.8 kGy for gamma-ray. Long lifetime is expected when using solid-state amplifiers for the CERN PS Booster RF system and PS damper system. R&D efforts have been continued to investigate the use of solid-state amplifiers for the RF feedback chain without radiation shielding. Another mixed-field irradiation test is planned for 2019.

ACKNOWLEDGMENT

We would like to thank S. Danzeca for identifying the cause of failure on the LDMOS. We wish to thank M. Shirakata, M. Yoshii, F. Tamura, K. Hasegawa and J-PARC Ring RF Group for their supports for beam test. We also would like to thank R. Gaillard, S. Gilardoni, M. Brugger, G. Spieza, the CERN CHARM support group and the CERN RF group for helping us with beam tests. This work was supported by JSPS KAKENHI Grant Number, JP18K11930 and Facility-service system of QST Takasaki, 2018A-C29.

REFERENCES

[1] M. Meddahi *et al.*, "LIU Technical Design Report - Volume I: Protons," CERN-ACC-2014-0337, 2015.
[2] ——, "LIU Technical Design Report - Volume II: Ions," CERN EDMS LIU-PM-RPT-00257, 2016.
[3] G. Arduini *et al.*, "Beam parameters at LHC Injection," CERN-ACC-2014-0006, 2014.
[4] D. Valuch, "Radio frequency systems of the CERN synchrotron accelerators ," in *Proceedings of 19th International Conference Radioelektronika, IEEE Conferences*, 2009, pp. 17–24.
[5] C. Ohmori *et al.*, "Development of a high gradient rf system using a nanocrystalline soft magnetic alloy," *Phys. Rev. ST Accel. Beams*, vol. 16, no. 11, p. 112002, Nov 2013.
[6] Y. Yoshizawa, "Common mode choke cores using the new fe]based alloys composed of ultrafine grain structure," *J. Appl. Phys.*, vol. 10, no. 64, p. 6047, Mar 1988. [Online]. Available: http://dx.doi.org/10.1063/1.342150
[7] "Nanocrystalline soft magnetic material, finemet." [Online]. Available: http://www.hitachi-metals.co.jp/prod/prod02/pdf/hl-fm9-e.pdf
[8] M. Paoluzzi, "Design of the PBS wideband RF system," CERN-ACC-NOTE-2013-0030, 2013.
[9] H. Damerau *et al.*, "Excitation of Longitudinal Coupled-bunch Oscillations with the Wide-band Cavity in the CERN PS," in *Proceedings of 7th International Particle Accelerator Conference (IPAC16)*, 2016, pp. 1724–1726.
[10] M. Paoluzzi and H. Damerau, "Design of the PS longitudinal damper," CERN-ACC-NOTE-2013-0019, 2013.
[11] H. Damerau and L. Ventura, "Longitudinal Coupled-Bunch Instability Studies in the PS," in *Proceedings of the Injector MD Days*, 2017, pp. 59–62.
[12] J. Saraiva and M. Brugger, "Radiation Levels at CERNs Injectors and their Impact on Electronic Equipment," CERN-ACC-2015-091, 2015.
[13] G. Favia, "Design report of a 1kW power amplier for the PS RF 10MHz system," CERN-ACC-NOTE-2018-0048, 2018.
[14] D. Grier, "The PS 10 MHz Cavity and Power Amplifier," PS/RF Note 2002-073, 2002.
[15] G. Spiezia *et al.*, "The LHC Radiation Monitoring System RadMon," in *Proceedings of 10th International Congress on Large Scale Applications and Radiation Hardness of Semiconductor Detectors*, 2011.
[16] "Methods for the calculation of radiation received and its effects, and a policy for design margins," ECSS E-ST-10-12C.
[17] J. L. Titus, "An Updated Perspective of Single Event Gate Rupture and Single Event Burnout in Power MOSFETs ," *IEEE Trans. Nucl. Sci.*, vol. 60, no. 3, pp. 1912–1928, Jun 2013.
[18] J. L. Titus *et al.*, "Impact of Oxide Thickness on SEGR Failure in Vertical Power MOSFETs; Development of a Semi-Empirical Expressiont," *IEEE Trans. Nucl. Sci.*, vol. 42, no. 6, pp. 1928–1934, Dec 1995.
[19] D. Fleetwood, "Evolution of Total Ionizing Dose Effects in MOS Devices with Moores Law Scaling," RADECS short course, 2017.
[20] T. R. Oldham and F. B. McLean, "Total ionizing dose effects in MOS oxides and devices," *IEEE Trans. Nucl. Sci.*, vol. 50, no. 3, pp. 483–499, Jun 2003.

[21] J. R. Schwank *et al.*, "Radiation effects in MOS oxides," *IEEE Trans. Nucl. Sci.*, vol. 55, no. 4, pp. 1833–1853, Aug 2008.
[22] J. Mekki, "A Mixed Field Facility at CERN for Radiation Test: CHARM," in *Proceedings of 15th European Conference on Radiation and Its Effects on Components and Systems (RADECS) , IEEE Conferences*, 2015, pp. 1–4.
[23] "The charm facility." [Online]. Available: https://charm.web.cern.ch/CHARM/
[24] G. Spiezia, "A New Radmon Version for the LHC and is Injection lines," *IEEE Trans. Nucl. Sci.*, vol. 61, no. 6, pp. 3424–3431, 2014.
[25] C. Ohmori and M. Paoluzzi, "RF Amplifier using VRF151G and BLF 574 Power RF Mosfets," CHARM Radiation Test Report, 2017.
[26] S. Danzeca, "Radiation Test Report at PSI," CERN-EDMS-2037116/1.
[27] E. K. F. Inanlou and J. Cressler, "An Investigation of Total Ionizing Dose Damage on a Pulse Generator Intended for Space-Based Impulse Radio UWB Transceivers ," *IEEE Trans. Nucl. Sci.*, vol. 60, no. 4, pp. 2605–2610, Aug 2013.
[28] D. C. Howard *et al.*, "An 816 GHz SiGe Low Noise Amplifier With Performance Tuning Capability for Mitigation of Radiation-Induced Performance Loss ," *IEEE Trans. Nucl. Sci.*, vol. 59, no. 6, pp. 2837–2846, Dec 2012.
[29] U. Dorda *et al.*, "Status of the MedAustron Ion Beam Therapy Centre ," in *Proceedings of the first International Particle Accelerator Conference (IPAC 12)*, 2012, pp. 4077–4079.
[30] M. Kanazawa *et al.*, "RF CAVITY WITH CO-BASED AMORPHOUS CORE," in *Proceedings of EPAC2006*, 2006, pp. 983–985.